9 Effects of stress relaxation on the microstructure of fresh Pd thin films

9.1 Introduction

The deposition (by CVD, sputtering, electro and electroless methods) of Pd onto a substrate leads to a composite structure including large amounts of extra energy. Part of the excess energy in these fine grain films is stored as microstrains and surface energy, which is released by the growth of Pd grains at high temperatures. Tschöpe at al. (1992) showed, by calorimetric measurements, that thermal relaxation in freestanding Pt and Pd nanocrystalline samples prepared by inert gas condensation occurred in two stages. The first reduction in the total Gibbs free energy corresponded to the relaxation of internal strains and/or non equilibrium grain boundaries. The second reduction in the total Gibbs free energy corresponded to grain growth. The remnant excess energy in composite structures is due to film/substrate interactions and is stored as "intrinsic" stresses within the film. Intrinsic stresses are also released at high temperatures.

Yet, at high temperatures, new stresses (thermal stresses) appear due to the difference in the thermal expansion coefficient of the metal and the substrate. In addition to thermal stresses, H_2 stresses will appear upon H_2 dissolution within the Pd lattice when the membrane is exposed to H_2 atmosphere. The resulting Pd lattice expansion is constrained by the support, which does not expand, and stresses build up within the film. Thermal

stresses and H_2 stresses are "extrinsic" stresses since they involve parameters outside the boundaries limiting the Pd thin film.

When the appropriate amount of energy is given to the composite system (Pd/substrate + H_2), microstrains, "intrinsic" and "extrinsic" stresses are released inducing changes in the microstructure within the Pd thin film. The changes in microstructure resulting from stress release can cause a composite Pd membrane to fail.

The main objective of the experiments described in this chapter was to investigate the stresses and their release occurring in composite Pd-PH structures. Specifically, the parameters affecting H_2 stresses were studied. In addition, the Pd microstructure and its changes with temperature were correlated with Pd grain growth, microstrains and stress release using diffraction techniques. Finally, the total stress in a composite Pd membrane was calculated for temperature and pressure conditions similar to conditions during membrane characterization.

9.2 Stress theory

9.2.1 Thermal stresses

The coefficients of thermal expansion of Pd and the substrate can be considered as linear functions of temperature within the temperature range (20-600ºC) considered in this study. Hence, the thermal stress (σ_{th}) along the Pd/substrate interface direction to which the thin film is subjected can be approximated by Equation (9-1) (Koch, 1994).

$$\sigma_{th} = \frac{(L_{sub} - L_{film}) \cdot \Delta T \cdot E_{film}}{1 - \nu} \qquad (9\text{-}1)$$

where L_{sub} and L_{film} are the thermal expansion coefficients of the substrate and the thin film respectively, ΔT the increment in temperature from a reference T_0 (T_0 = 20ºC), E_{film}

is Young's modulus and ν the Poisson's ratio of the metal film. According to Equation (9-1), thermal stresses are a linear function of temperature. However, the linear character of thermal stresses with temperature is only observed in the elastic region of the metal. When the thermal stresses exceed the elastic limit of the film they are released by plastic deformations.

9.2.2 H_2 stresses

H_2 stresses are equal to the H_2 strain times Pd Young's modulus (E_{film}) and are given by Equation (9-2)

$$\sigma_H = \varepsilon_H \cdot E_{film} \tag{9-2}$$

where ε_H, is the H_2 strain, which was derived from experimental data reported by (Baranowski et al., 1971). Baranowski et al. (1971) found the volume increase due to interstitial H_2 to be a unique and linear function of n(H/Pd) for many fcc metals and alloys (Pd, Pd-Ir, Pd-Au, Pd-Ag, Pd-Pt and Pd-Cu) regardless of the initial lattice volume and the hydride phase (α or β). The linear volume increase as a function of n(H/Pd) holds for 0<n<0.7 and is shown in Equation (9-3).

$$\Delta V = (a^3 - a_0^3) = 11.56 \cdot n(H/Pd)^{1} \tag{9-3}$$

where ΔV is the volume increase of the lattice cell in $Å^3$, a is the lattice parameter in Å and n(H/Pd) the H_2 content. a_0 is the metal lattice parameter in inert atmosphere. Hence, the increase in the lattice parameter is given by Equation (9-4)

$$a = (11.56 \cdot n(H/Pd) + a_0^3)^{1/3} \tag{9-4}$$

[1] Equation (9-3) was derived by measuring ΔV and n(H/Pd) on the graphic reported by Baranowski et al. (1971)

Performing a Taylor expansion around n(H/Pd)=0 to the first order leads to Equation (9-5)

$$a \approx a_0 + \frac{1}{3} \cdot \frac{11.56}{(a_0^3)^{\frac{2}{3}}} \cdot n(H/Pd) + o(n(H/Pd)) \tag{9-5}$$

Substituting a_0 with the value for Pd (a_0=3.889Å) leads to Equation (9-6)

$$\frac{a - a_0}{a_0} = \frac{1}{3} \cdot 0.19 \cdot n(H/Pd) \tag{9-6}$$

Equation (9-6) was also derived by Eastman et al. (1993), which found the same expression for ε_H vs. n(H/Pd). Hence, the H_2 stress is a linear function of the H_2 content, n(H/Pd) within an elastic region. Stresses will also be released if the elastic limit of the metal is exceeded.

9.2.3 Stresses in a composite Pd/substrate structure

The total stress in a composite Pd/substrate structure is the sum of all stresses. A composite Pd membrane under reaction conditions will be subjected to the total stress (σ_{total}) given by Equation (9-7)

$$\sigma_{total} = \sigma_{th} + \sigma_H = [\frac{(L_{sub} - L_{film}) \cdot \Delta T}{1 - \nu} + \frac{k_H}{3} \cdot n(H/Pd)] \cdot E_{film}$$
$$with \tag{9-7}$$
$$k_h = 0.19 \pm 0.01$$

9.3 Experimental

9.3.1 The preparation of samples

The composite Pd membranes listed in Table 3-2 have a very small thickness compared to the outside diameter (OD) of the cylindrical substrate. Hence, any composite Pd membrane can be considered as a flat thin film and the study of stresses can be undertaken using small flat porous plates covered with a Pd film with the same thickness.

0.2μm grade PSS plates (1.5cm^2, 1mm thick), 0.5μm grade PH plates (1.5cm^2, 1mm thick) and α Al_2O_3 supports (1.5cm^2, 2mm thick) were cleaned according to the procedure described in Section 3.1.1. PSS plates were oxidized at 600ºC for 12 hr. PH plates were oxidized at 900ºC for 12 hr to ensure the formation of a thick Cr_2O_3 layer. Activation and Pd deposition were performed as described in Section 3.1.1. For the bimetallic Cu-Pd-PH samples, Cu was deposited by the electroless plating method using plating baths listed in Table 7-1. The thickness and Cu content of each layer was determined by the gravimetric method. After the metal deposition the Pd-Cu samples were annealed in UHP H_2 atmosphere at 650ºC for 24 hr. Two different Cu-Pd-PH samples were considered for stress calculation: Pd/Cu-40wt% (sample Pd-Cu-4), Pd/Cu-41wt% (sample Pd-Cu-5) and Pd/Cu-13wt% (sample Pd-Cu-6). Samples studied in this chapter are listed in Table 9-1.

Table 9-1 List of samples studied in this chapter.

Sample	Pd thickness, L (μm)	Pressure (bar), atmosphere	Temp. range (ºC)	Experiment description
PH-1a ("fresh")	12	1, He	25-600	Measurement of microstrains, Pd grain size, Pd lattice parameter (a) and stresses as temperature was increased
PH-1b	12	1, He	60-400	Measurement of microstrains and stresses of a heat-treated sample as temperature was increased
PH-1c	12	1.5, H_2	60-500	Measurement of stresses as a function of H_2 concentration in the Pd layer (n=H/Pd)
PH-2a (Pre-treated in He at 400ºC for 1 hr)	12	1, He	60-400	Measurement of stresses in a pre annealed sample. Comparison with PH-1b
PH-3a (Pre-treated in He at 400ºC for 1 hr)	12	1, He	300-500	Measurement of stresses in a pre annealed sample at T>400.
PH-4a (Pre-treated in He at 400ºC for 1 hr)	12	1, He⇆1.5 H_2 5 times switching	50	Effect of atmosphere switching on microstrains and Pd morphology
Al_2O_3-1a ("fresh")	10	1, He	20-500	Microstrains release as a function of temperature in He
Al_2O_3-2a ("fresh")	10	1, H_2	20-500	Microstrains release as a function of temperature in H_2
Al_2O_3-3a/4a/5a/6a ("fresh")	6	1, H_2	300/400/500/600	Pd microstructure after annealing in H_2 for 48 hr at 300 (Al_2O_3-3), 400 (Al_2O_3-4), 500 (Al_2O_3-5) and 600ºC (Al_2O_3-6)
PSS-1a ("fresh")	10	-	-	Pd microstructure of a fresh Pd thin film
PSS-1a ("fresh")	10	1, H_2	500	Pd microstructure after heat-treatment at 500ºC for 48 hr in H_2
Pd-Cu-5	PH	1, He	20-400	Stress measurements in PdCu –PH composite structures (β phase)
Pd-Cu-6	PH	1, He	20-400	Stress measurements in PdCu –PH composite structures (α phase)

The letter following the sample number designates the experiment. For instance, PH-1b stands for "sample PH-1, second experiment". "Fresh" samples are the ones which were only dried at 120ºC overnight before any experiment. Only samples PH-2a, PH-3a and PH-4a were pre-treated in He atmosphere at 400ºC for one hour to release initial microstrains and "intrinsic" stresses present in every "fresh" Pd film.

9.3.2 X-ray diffraction procedures

9.3.2.1 X-ray diffractometers

Diffraction data were collected using Cu-Kα radiation on a PANalytical X'Pert Pro MPD located at the High Temperature Materials Laboratory (HTML) in Oak Ridge National Laboratory (ORNL), Oak Ridge, Tennessee. Parallel-beam optics, consisting of an incident-side graded multilayer parabolic X-ray mirror and a diffracted-side 0.09° parallel-plate flat collimator, were used to alleviate errors associated with sample displacement. Samples were loaded into an Anton Paar XRK900 reaction chamber which allowed the temperature to be varied between 25 and 900 °C and the gas environment to be varied between 1 and 1.5 atm of He or He-4%H_2 (static or flowing).

All experiments listed in Table 9-1 were performed on the PANalytical diffractometer except for Al_2O_3-1a and Al_2O_3-2a. Diffraction data of experiments Al_2O_3-1a and Al_2O_3-2a were collected with the time resolved HTXRD diffractometer already described in section 3.4.2.1.

9.3.2.2 Microstrains-size separation: the Williamson-Hall method

In metals, two types of strains (% of elongation, $(d-d_0)/d_0$) can be encountered: non-uniform strains (microstrains) and uniform strains (macrostrains). Non-uniform strains

are pictured as a distribution of d-spacings and lead to XRD peak broadening while uniform strains, which arise from "intrinsic" and "extrinsic" stresses, lead to XRD peak shifting. This section deals with the determination of microstrains and grain size by XRD peak broadening measurements.

Not only microstrains lead to the broadening of XRD peaks (β_{total}) but also small grain sizes (<100nm), stacking faults and twins, and machine limitations contribute to the broadening of XRD peaks according to Equation (9-8)

$$\beta_{total} = \beta_{size} + \beta_{microstrains} + \beta_{faulting} + \beta_{machine} \quad (9\text{-}8)$$

The density of stacking faults and twins in fcc metals can be determined by measuring the shift of two pairs of reflections such as the (111)-(200) pair and the (222)-(400) pair (Warren and Averbach, 1950). However, several reports showed (by Transmission Electron Microscope (TEM) techniques) that thin films formed with a gentle deposition method such as electrodeposition, cold condensation and sputtering did not include severe defects in the atomic layers. Since electroless deposition involves a gentle chemical process the density of stacking faults and twins was considered to be negligible. Therefore, XRD peak broadening was considered to be only a function of crystallite size, microstrains and machine broadening according to Equation (9-9)

$$\beta_{total} = \beta_{size} + \beta_{microstrains} + \beta_{machine} \quad (9\text{-}9)$$

The contribution of machine broadening ($\beta_{machine}$) to the total peak broadening is readily measured using a standard Si or LaB_6 powder supplied by NIST. Equation (9-9) can then be easily reduced to Equation (9-10)

$$\beta_{total} = \beta_{size} + \beta_{microstrains} \quad (9\text{-}10)$$

Two approaches can then be undertaken to determine crystallite size and microstrains: the use of Williamson-Hall's method (Williamson and Hall, 1953) to separate grain size contribution from microstrains contribution or the use of the Warren-Averbach's method (Warren and Averbach, 1950) to measure simultaneously grain size, grain size distribution and microstrains. Warren-Averbach's method leads to consistent data when several orders of diffraction can be collected for a given set of planes, for instance when reflections (111), (222), (333) etc. are available. In conventional X-ray diffractometers with a Cu radiation source only 2 orders of diffraction are available for Pd making the use of Warren-Averbach's method unworthy. Therefore, microstrains-size separation in Pd deposits was performed using Williamson-Hall's method described in detail by Williamson and Hall (1953).

In Williamson-Hall's method the peak broadening (β), expressed in radians, was assumed to be the sum of a tan(θ) term for the microstrains, and a 1/cos(θ) term for the grain size as given in Equation (9-11)

$$\beta = 4e \cdot \tan(\theta) + \lambda_{Cu} / (t \cdot \cos(\theta)) \qquad (9\text{-}11)$$

where $e \approx (\Delta d/d)_{hkl}$ is an approximate upper limit of the maximum distortion, λ_{Cu} the Cu X-ray wavelength, t the grain size and θ the half peak position. Equation (9-11) can also be written as Equation (9-12)

$$\beta \cdot \cos(\theta) = \frac{\lambda}{t} + 4e \cdot \sin(\theta)$$
$$with \qquad (9\text{-}12)$$
$$e = 1.25 \cdot \sqrt{<\varepsilon^2>}$$

where $\sqrt{<\varepsilon>^2}$ is the root mean square strain (rms), which is a measurement of the Pd lattice distortion. Peak width (β) was determined by fitting every reflection with a Lor-

entz peak function after subtracting the $K\alpha_2$ component and the background. $\beta \cdot \cos(\theta)$ was then plotted as a function of $\sin(\theta)$ for all available reflections: (111), (200), (220), (311), (222), (400), (331) and (420). The plotted data were then fitted with a straight line, where the slope equaled $4e$ and the intercept with the "y" axis equaled λ_{Cu}/t.

9.3.2.3 Stress measurement: lattice strain Vs. $Sin^2\psi$ method

Diffraction data were collected from the (422) peak of Pd between 146 and 157°2θ at ψ tilts of 0, ±28.2, ±42, ±55°psi. The peak position, and ultimately the total stress in the sample, was determined using PANalytical X'Pert Stress by performing a routine which included absorption intensity correction, subtraction of linear background, Lorentz-Polarization correction, stripping of the Cu-$K\alpha_2$ peak, and then determining the peak position using a Lorentz fitting method. The variation of peak positions as a function of ψ tilt were then analyzed using a uniaxial $\sin^2\psi$ plot to determine the macrostrain within the plane of the coating. This macrostrain was converted to a stress using a Young's modulus of 133.52 GPa and a Poisson's ratio of 0.3847. The $\sin^2 \psi$ plot uses the change in peak position at different tilts of ψ to determine the macrostrain to which the sample is subjected within the surface plane of the sample.

9.4 Results and discussion

9.4.1 Microstructure of a fresh electroless plated thin Pd film

9.4.1.1 The morphology of fresh electroless Pd deposits

Figure 9-1 shows top view SEM micrographs of sample PSS-1a. The fresh, i.e. dried at 120ºC overnight, Pd coating had a "cauliflower" type of structure with different features. In the low magnification picture, Figure 9-1(a), shows large (70μm×50μm) agglomerates delimited by pronounced dark boundaries. One of these features, called "super structure" was framed in Figure 9-1(a). Figure 9-1(a) also shows that the "super structure" is characterized by features delimited with dark boundaries (black arrows) or light boundaries (circle). Figure 9-1(b) shows a high magnification SEM micrograph within the "super structure" framed in Figure 9-1(a). The "super structure" included Pd clusters, pointed by arrows in Figure 9-1(b), with sizes in the order of one micron. Pd clusters merged to form larger globules (encircled in Figure 9-1(b)) having sizes within 3-5μm. Most important was the very fine grain structure within a Pd cluster shown by Figure 9-1(c). The surface of a large Pd cluster (framed with a black square in Figure 9-1(c)) was in fact constituted of many small grains, which were considered to be Pd crystallites due to their small size (50-100 nm). The black arrow in Figure 9-1(c) points to a group of Pd crystallites.

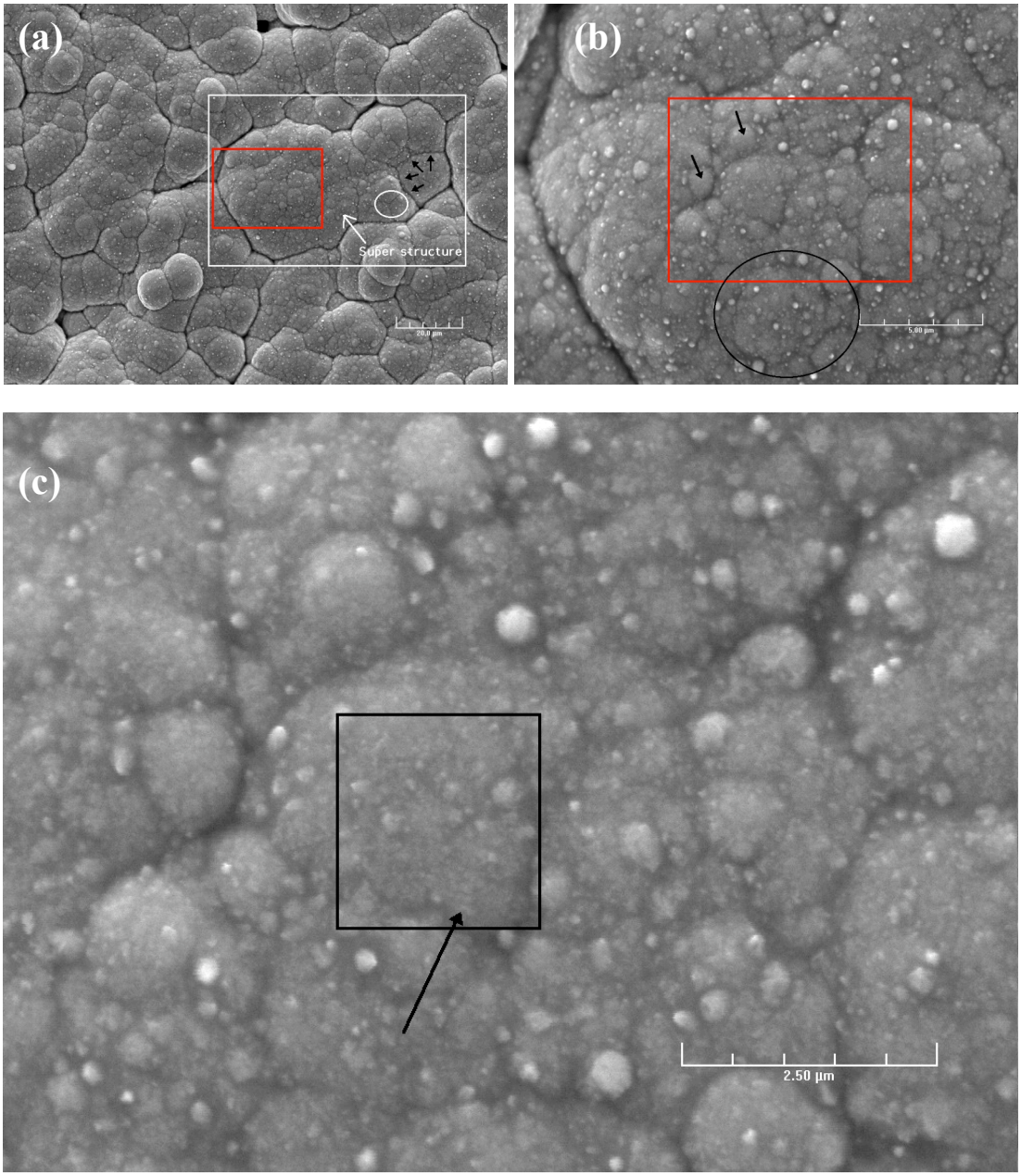

Figure 9-1 Surface structure of sample PSS-1a. (a) mag: 1kX, Pd "super structure" (b) mag: 5kX, Pd clusters and (c) mag: 10kX domains of crystallites in a Pd clusters. Red squares represent the area of the next picture.

Hence, fresh Pd deposits were characterized by a "cauliflower" structure with large structures delimited by pronounced boundaries, characterized by agglomerates of Pd clusters, which consisted of thousands of Pd crystallites having 50-100nm in diameter.

9.4.1.2 Initial Pd grain size, microstrains and "intrinsic" stresses

Using only Scherrer equation ($t_{hkl}=0.9\lambda/\beta\cos\theta$) on the (111) and (222) reflections led to t_{222} higher than t_{111} by a factor of two, which was also reported on Pd black when microstrains were not accounted for (Bogdanov et al., 1984). Hence, microstrains were also present in electroless Pd deposits. Therefore, the initial microstrains present in the fresh Pd film and initial Pd grain size were estimated by performing a strain-size separation on sample PH-1a using Williamson-Hall plot, shown in Figure 9-2(a). Initial rms equaled $2.9\cdot10^{-3}$ and initial Pd grain size equaled 97nm, which was in agreement with Pd grain size measured on SEM micrographs. It has been shown in the case of nanocrystalline Pd that microstrains decreased from 0.5% to 0.05% as crystallite size increased from 10nm to 100 nm (Sanders et al., 1995; Weissmuller et al., 1995). Based on Sander's and Weissmuller's findings it was hypothesized that since microstrains decreased with increasing grain size, microstrains were confined to small crystallites and/or shells adjacent to the interfaces within the crystallites (Reimann and Wurschum, 1997). The initial microstrains measured in PH-1a (0.29%) appeared to be higher than the values reported in the literature (0.05%) when the Pd grain size measured with SEM and XRD was around 100nm.

Figure 9-2(a) also shows that the (111) and the (222) reflections were considerably sharper than the (200) and (400) reflections, which was also noted by other researchers (Bogdanov et al., 1984; Reimann and Wurschum, 1997). Indeed, Reimann and Wur-

schum, (1997) and Bogdanov et al. (1984) also reported this unexpected anisotropic variation of β cos(θ) with respect to the reflection.

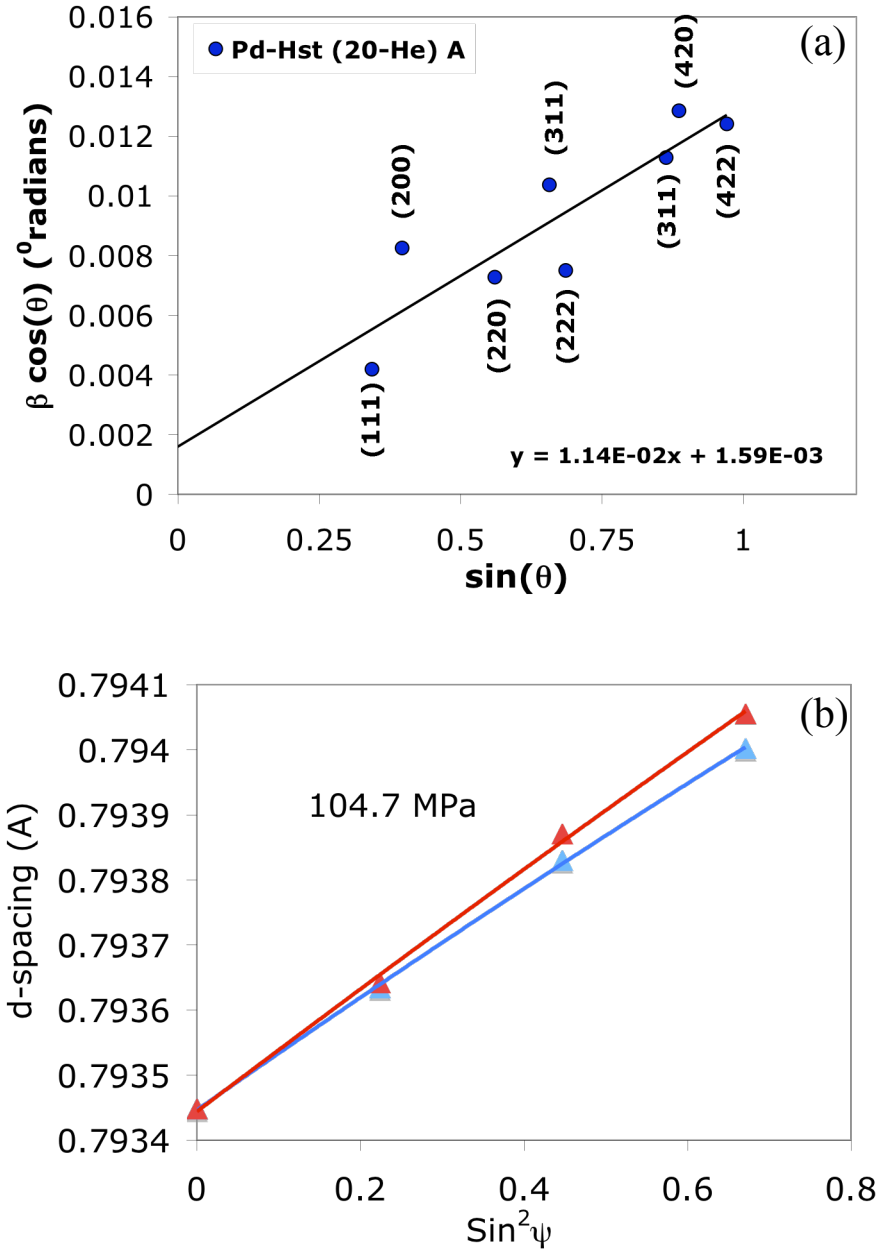

Figure 9-2 (a) Williamson-Hall plot of PH-1a sample. (b) Strain-sin$^2\psi$ plot for the same Pd coating. Data taken at 20°C.

The anisotropic variation of $\beta \cos(\theta)$ indicated that either grains were longer along the [111] direction than along the [200] direction or that a high density of stacking faults and twins was present along the [200] direction. According to Reimann and Wurschum, (1997) neither the high density faults nor the anisotropic grain shape hypothesis were compatible with Pd crystallite shape from high resolution TEM investigations. Hence, they postulated that the large variations of $\beta \cdot \cos(\theta)$ with respect to the peak reflection were due to the anisotropic elasticity factor of Pd. They plotted $\beta \cdot \cos(\theta)$ as a function of $\sin(\theta)/E_{hkl}$ (E_{hkl} is the Pd Young's modulus for the hkl reflection) and found a straight line. Therefore, the anisotropy seen in Figure 9-2(a) was due to the anisotropy in Pd elasticity.

The initial "intrinsic" stresses of the fresh PH-1a sample were determined using d-$\sin^2\psi$ experimental data plotted in Figure 9-2(b). An initial tensile stress of 104.7±9 MPa was measured along the y direction. The tensile nature of the initial stress can be explained by the high melting point of Pd and the low temperature (60ºC) at which the deposition was carried out.

Indeed, during Volmer-Weber growth, the nature of the initial "intrinsic" stresses depends on the mobility of the metal being deposited. The mobility of the metal depends on its melting point (the concept of Tamman temperature) and the temperature of the substrate at which the deposition is performed. Therefore, the initial "intrinsic" stress of a fresh coating depends on the $T_{substrate}/T_{melt}$ ratio and, given a substrate temperature, metals are categorized in low-mobility ($T/T_m<0.2$) and high mobility ($T/T_m>0.2$) metals (Koch, 1994). Low mobility metals show tensile stresses during deposition. Moreover, the tensile stress increased linearly with film thickness. These stresses are mostly located at the grain

boundaries. In the particular case of Pd deposited at a temperature of 60ºC, the T/T_m ratio (333K/1823K) equaled 0.18, so that Pd can be considered as a low mobility metal, which was in agreement with the tensile nature of the initial stress of the coating.

Grain boundaries are known to be sources of intrinsic stresses and according to Hoffman "*the inter-atomic forces at the grain boundaries tend to close any existing gap, with the result that the neighboring crystallites are strained in tension*"[1]. Weissmuller and Lemier, (1994) also reported that grain boundary stress in Pd-H tended to expand the crystal lattice.

[1] Citation from Koch (1994).

9.4.2 Pd microstructure changes with temperature

9.4.2.1 Morphology changes with temperature

Figure 9-3(a), (c) and (e) show the Pd morphology of PSS-1a at 1000X, 5000X and 10000X respectively. Figure 9-3(b), (d) and (f) show the Pd morphology, at the same magnifications, of a thin Pd film after heat-treatment at 500ºC for 48 hr in H_2 (PSS-2a). Figure 9-3(b) shows that after treatment at 500ºC the boundaries between "super structures" were less pronounced than the same boundaries in the fresh sample. The change in appearance of pronounced boundaries between large structures can be better seen in Figure 9-3(d). The black arrows in Figure 9-3(d) point to boundaries between large structures, where some sintering can be clearly seen. Figure 9-3(d) also shows that Pd clusters, and Pd grains inside "super structures" sintered after heat-treatment leading to a relatively uniform microstructure within each "super structure" having Pd grains as large as 0.5-1μm. The large Pd grains formed upon heating can be clearly seen in Figure 9-3(f) pointed out by the arrows.

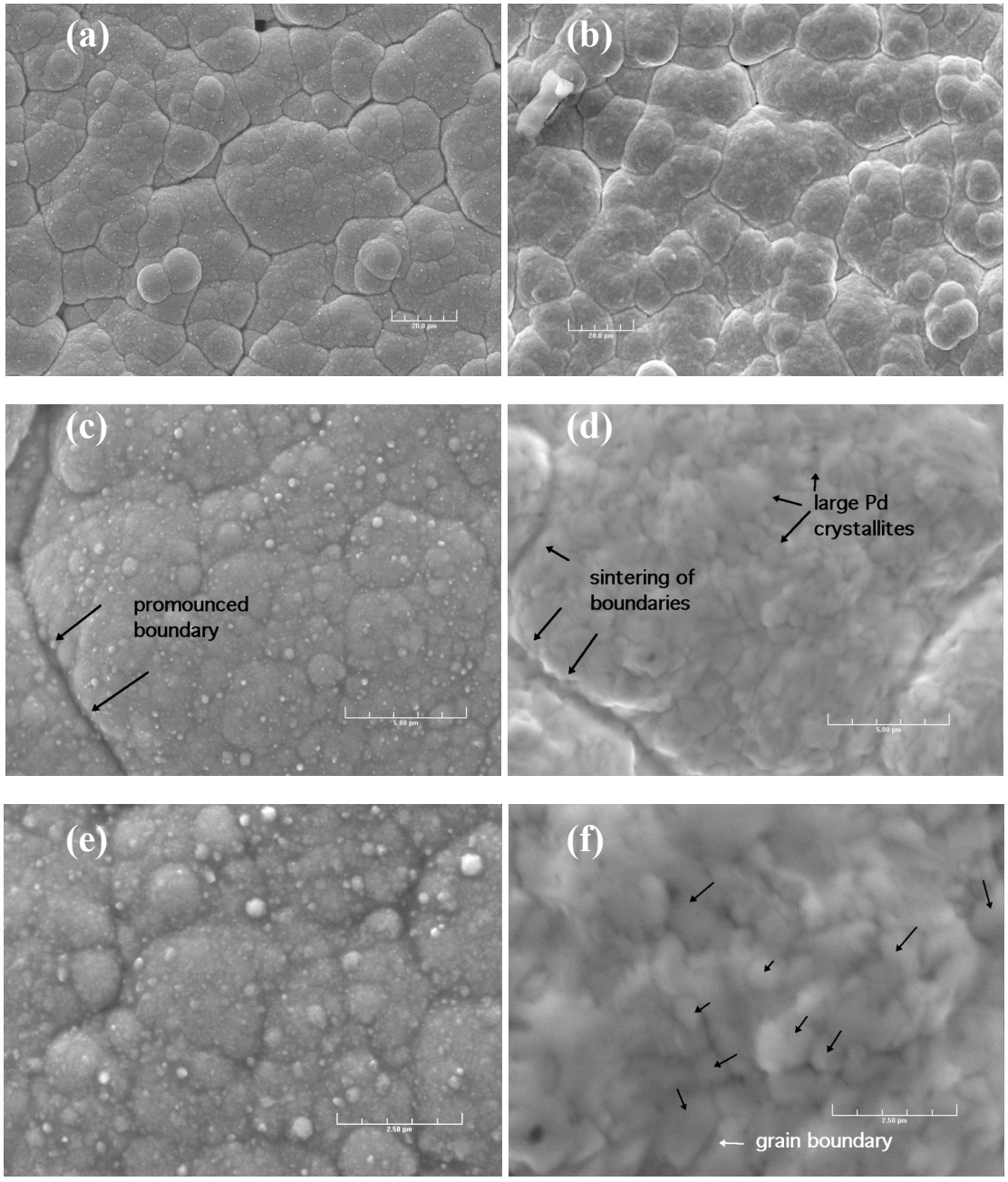

Figure 9-3 surface pictures of PSS-1a (a) mag.: 1kX, (c) mag.: 5kX and (e) mag.: 10kX. Surface microstructure of PSS-2a (upon heating at 500ºC for 48 hr) is shown at (b) mag.: 1kX, (d) mag.: 5kX and (f) mag.: 5kX. mag1KX, scale bar: 20 μm, mag 5KX scale bar: 5 μm and mag 10KX scale bar:2.5 μm.

Pd layers (6μm thick) were deposited on α-Al_2O_3 supports and annealed at different temperatures (300, 400, 500 and 600ºC) for 48 hr in H_2. The morphology of the annealed Pd layers (samples Al_2O_3-3a/4a/5a/6a), studied by SEM, is shown in Figure 9-4(a)(b)(c) and (d) respectively. No significant changes were noticed in the shape of clusters for the samples annealed at 300 and 400ºC. Indeed, the clusters in both samples had similar size and sharp edges. Pd clusters in the 500ºC annealed sample did not show sharp edges indicating that Pd grain and Pd cluster sintering process started at a temperature between 400 and 500ºC. At 600ºC Pd clusters were hardly discerned, instead, a distinguished uniform Pd layer with Pd grains as large as 5μm were present.

9.4.2.2 Grain growth and microstrains release with temperature

Figure 9-5 shows the Williamson-Hall plot of sample PH-1a annealed in He atmosphere at different temperatures (400, 500 and 600ºC). Experimental data obtained at 20ºC, "(20-He) A", was also added for comparison purposes. At high temperatures (>400ºC), plotting $\beta \cdot \cos(\theta)$ as a function of $\sin(\theta)$ led to a straight line having a very low slope value (rms=$3.2 \cdot 10^{-4}$) and passing through the origin indicating that microstrains, initially present in the Pd deposit, were released (0.03% at high temp.) and that grains grew very large. Performing the microstrains-size separation at room temperature after heat-treatment, "(20-He) B" filled circles, led to the same results found at high temperatures. Therefore, initial microstrains were irreversibly released after treatment in He atmosphere at 400ºC for one hour.

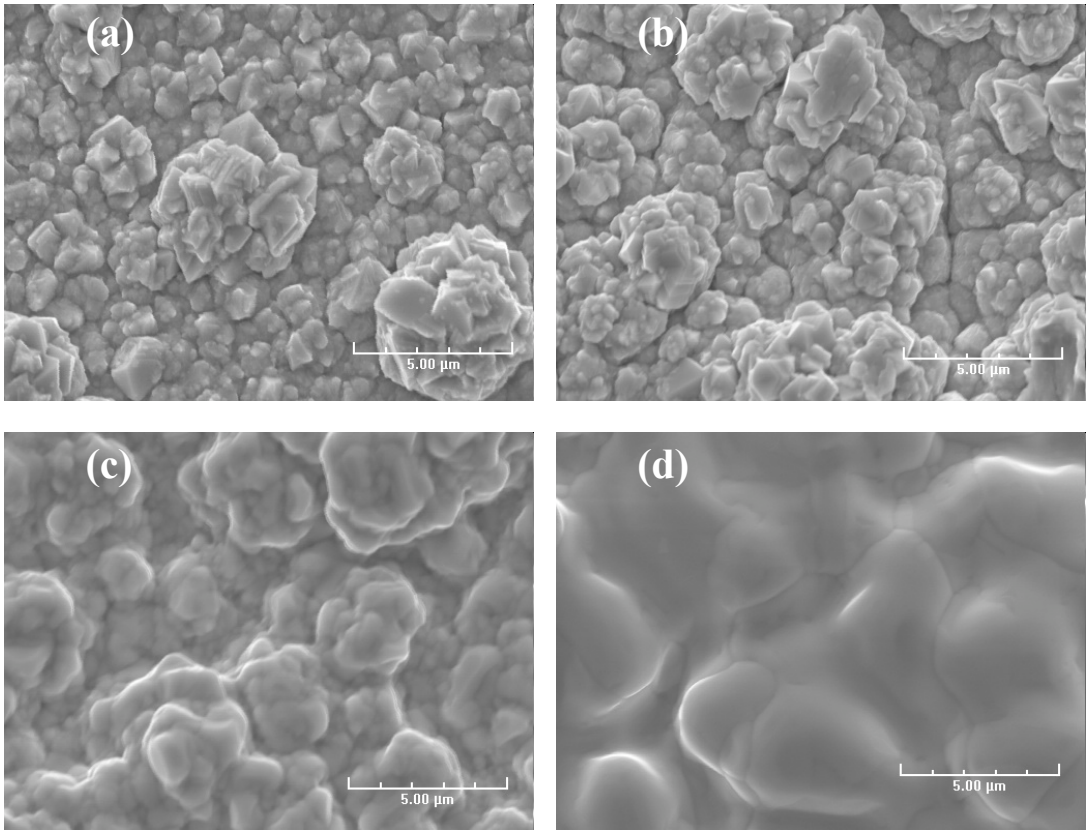

Figure 9-4 Pd-α -Al_2O_3 deposits annealed in H_2 at (a) 300 (Al_2O_3-3a), (b) 400 (Al_2O_3-4a), (c) 500 (Al_2O_3-5a) and (d) 600ºC (Al_2O_3-6a) for 48 hr (Mag 5000)

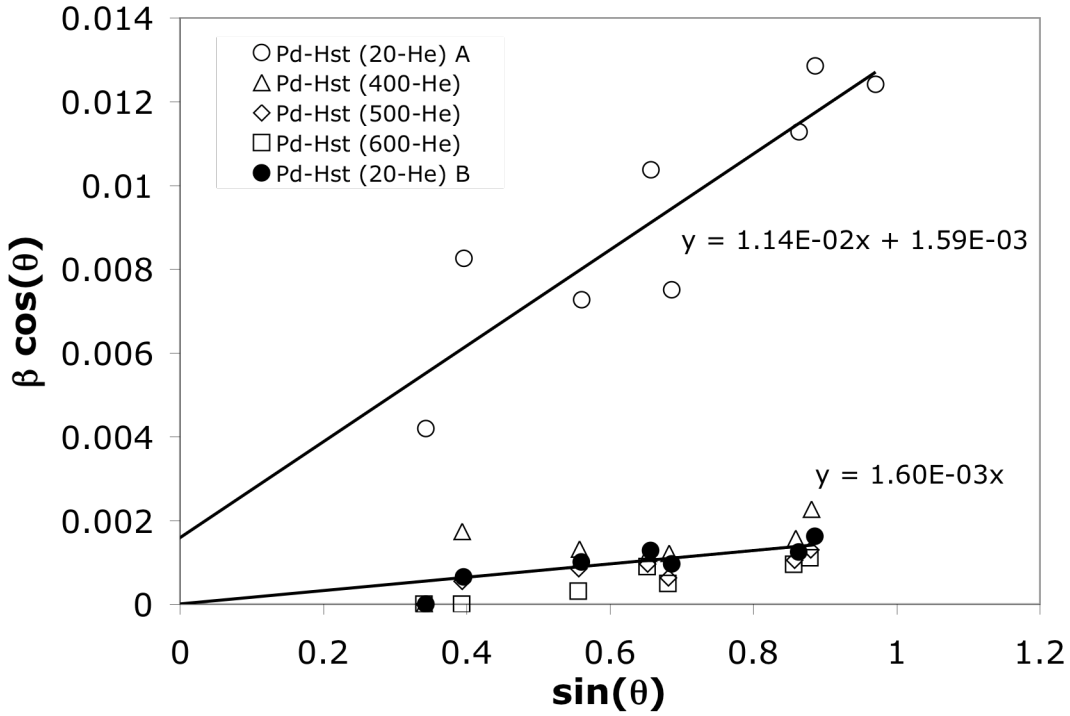

Figure 9-5 Strain-size separation for PH-1a at different temperatures. Letters A and B correspond to the scan at room temperature before high temperatures (A) and after high temperatures exposure treatment (B).

Since Pd grains were initially large (100nm) peak broadening was primarily due to microstrains in the Pd lattice. The peak broadening (FWHM or β) of the (111), (200), (220), (311) and the (222) reflections was followed as a function of temperature in He atmosphere for sample Al_2O_3-1a (pure Pd thin film). The experiment consisted of collecting x-ray data for all reflections while the temperature was increased at a rate of 3ºC/min. Figure 9-6 shows that the FWHM of all reflection, except the (111) reflection, reached the machine-broadening limit (0.1°) at temperatures higher than 350ºC, that is, above 350ºC in He atmosphere, all microstrains initially present in the thin film were released, which was in agreement with experiment PH-1a.

Microstrains release in H_2 atmosphere is shown in Figure 9-7 as a function of time at 200, 300, 400 and 500ºC for sample Al_2O_3-2a (pure Pd thin film). The experiment consisted of collecting x-ray data for all reflections as a function of time at a given temperature. The temperature was increased by 100ºC increments. In H_2 atmosphere, Pd reflection peaks (except the (111) reflection) were still broad at 400ºC, however, at 500ºC peaks sharpened readily and the FWHM of all peaks reached the machine broadening limit. Moreover, at each temperature equal to or below 400ºC, some microstrains release occurred in the first 60 minutes after which strains reached a constant value. Therefore, it appeared that microstrains release mechanism took place at a faster rate in He atmosphere than in H_2 atmosphere, which was due to the adsorbed H atoms along the grain boundaries.

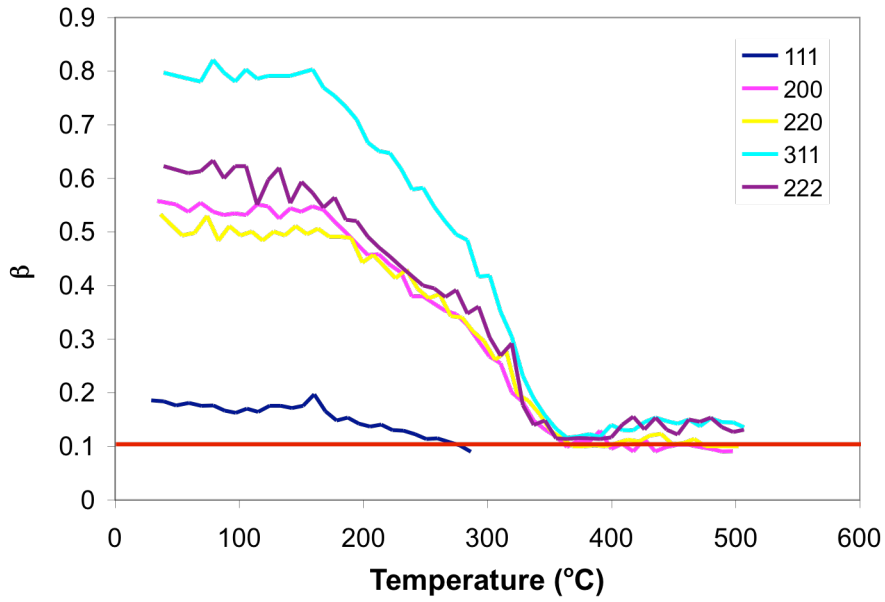

Figure 9-6 Microstrains release in He atmosphere in sample Al_2O_3-1a as a function of temperature. Heating rate 3°C/min.

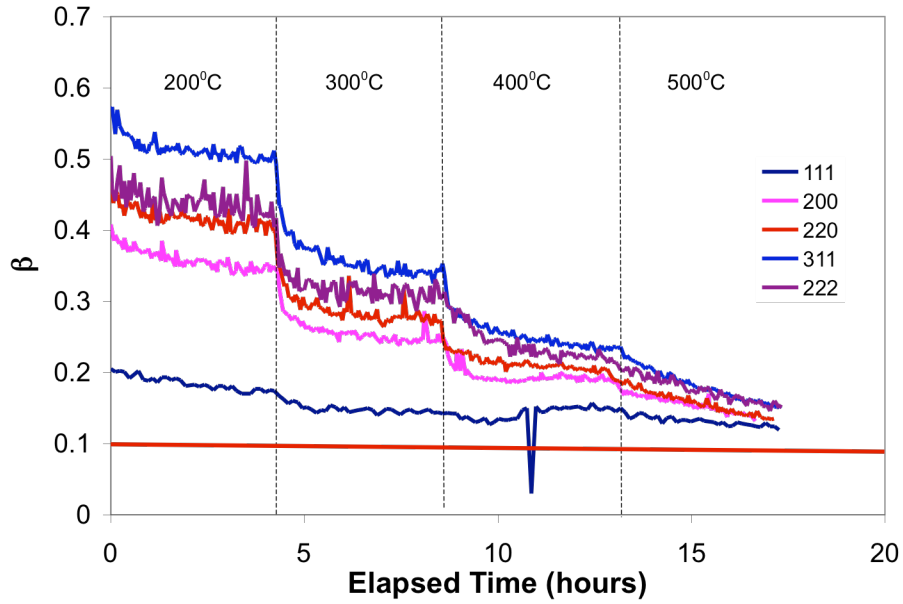

Figure 9-7 Microstrains release as a function time for sample Al_2O_3-2a in H_2 atmosphere at 200, 300, 400 and 500°C.

The study of Pd grain growth was not possible since their size was already large (100nm) at the "fresh" stage. However, according to Tschöpe et al. (1992), grain growth occurs after microstrains are released, therefore, Pd grain growth in electroless plated films started to occur at temperatures ranging between 350-400ºC depending on the atmosphere. The hypothesis that Pd grains started to grow at T>350-400ºC can be substantiated by the fact that, as seen in Figure 9-4(b), no significant structure modification occurred at 400ºC in H_2 atmosphere.

9.4.2.3 "Intrinsic" and "extrinsic" stresses release with temperature

Upon heating sample PH-1a, "extrinsic" thermal stresses were added to the already existing "intrinsic" stress. The total stress in sample PH-1a was measured at several temperatures (250, 400, 500 and 600ºC) in He atmosphere. Figure 9-8 shows the total stress to which the thin Pd film was subjected as a function of temperature. Initially, before any treatment at high temperatures, the film was under a tensile stress of 104.7 MPa. At temperatures higher than 250ºC, the thin film was subjected to compressive stresses. The magnitude of the compressive stresses was equal to 25 MPa at 250ºC and 400ºC and 13MPa at 500ºC and 600ºC as seen in Figure 9-8. When cooled to room temperature (25°C), after the high temperature treatment, the thin film was back under a tensile stress although the magnitude of the tensile stress was lower (41 MPa) than the value at the "fresh" state (104.7 MPa).

The difference in the tensile stress before and after exposure to high temperatures indicated that the initial "intrinsic" stress was released. In fact, stress release started at a temperature between 250 and 400ºC since the film was under the same compressive stress at those two temperatures.

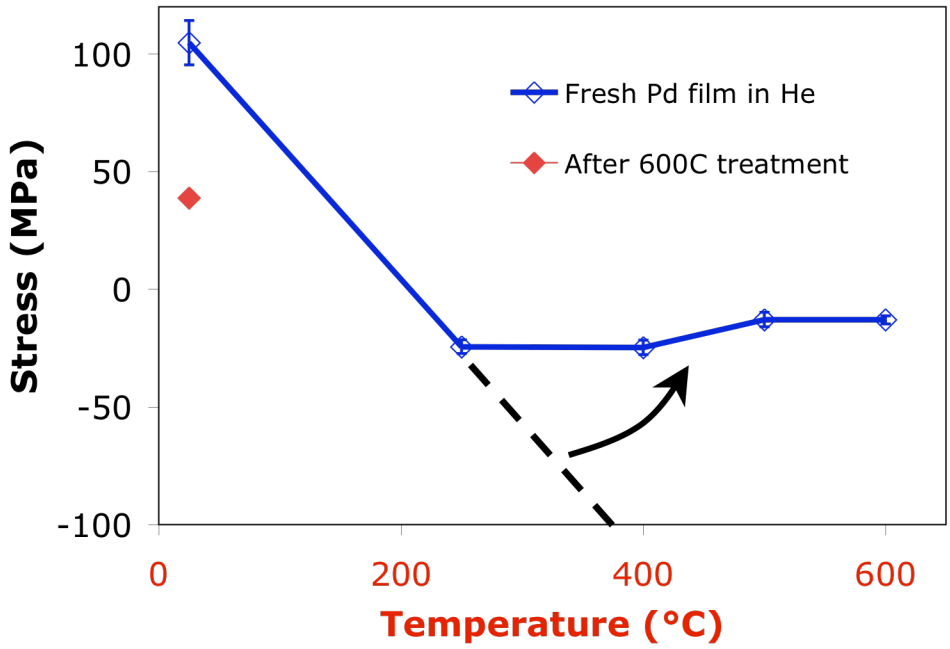

Figure 9-8 Stress release in sample PH-1a as a function of temperature

Further stress release occurred at 500ºC since the film was under a less compressive stress than at 400ºC. The stress-temperature plot seen in Figure 9-8 was characteristic of the first high temperature treatment of the "fresh" PH-1a sample where the initial stresses were released by dislocations in the metal.

The stress-temperature plot during the temperature treatment of sample PH-1b is shown in Figure 9-9 (diamonds). During the heat-treatment of sample PH-1b, the stress was found to be, within the temperature-range studied (60-400ºC), a linear function of the temperature as predicted by Equation (9-1). The negative slope indicated that the thin Pd film expanded more than the PH substrate by $1.25 \cdot 10^{-6}$ m/(m K). Since, the thermal stress was a linear function of temperature, the elastic region for a Pd sample annealed at 600ºC was found to be 60-400ºC.

In order to better understand the release of stresses that occurred during the heat-treatment of sample PH-1a, sample PH-2a was pre-treated in He atmosphere at 400ºC for one hour to release the initial microstrains and the initial stress present in the film. The total stress of sample PH-2a was then measured at 60, 200 and 400ºC and is also plotted in Figure 9-9 (squares). As seen in Figure 9-9, the total stress-temperature function of PH-2a corresponded to the same stress-temperature function of sample PH-1b, which indicated that the heat-treatment at 400ºC was sufficient to release the initial tensile stress. Furthermore, the elastic region of a thin Pd film annealed at 400ºC was also found to be 60-400ºC. Sample PH-3a, also pre-treated at 400ºC for one hour in He, was studied in order to elucidate the thermal stress at temperatures higher than 400ºC.

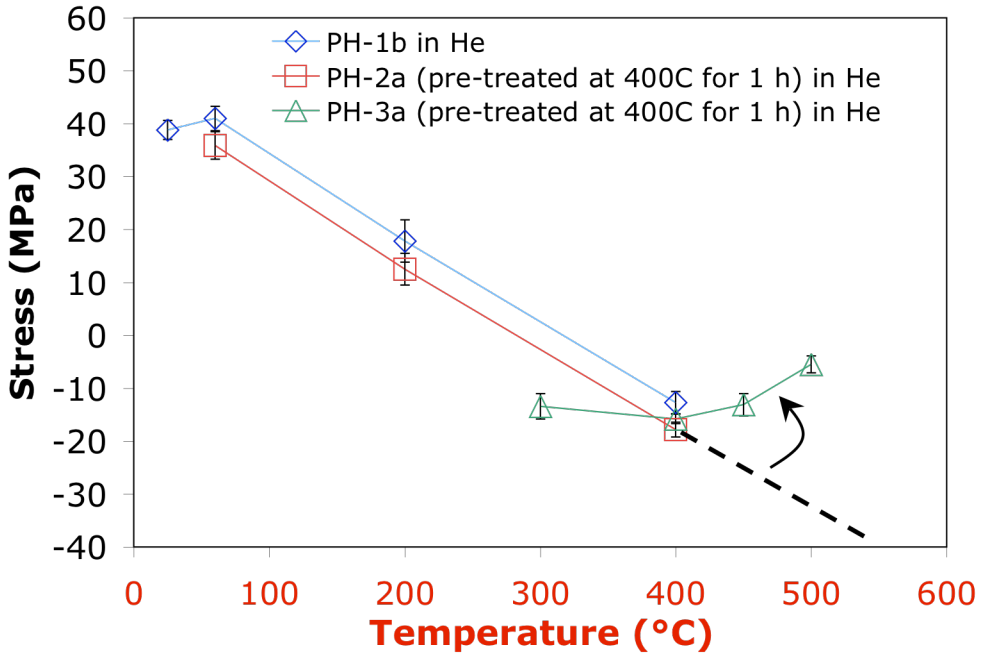

Figure 9-9 Stress in thin Pd films as a function of temperature. (◇) PH-1b, (□) PH-2a and (△) PH-3a.

Figure 9-9 shows the thermal stress vs. temperature behavior shown by sample PH-3a (triangles) in the 350-500ºC temperature range. The stress at 350 and 400ºC was similar to the stress shown by samples PH-1b and PH-2a at the same temperatures.

However, at 450ºC thermal stress started to relax and at 500ºC compressive stresses were totally released (-2.7MPa) as a result of plastic deformations. Hence, the elastic region of thin Pd films annealed at 400ºC was found to be 20-400ºC and thermal stress within the determined elastic region were given by Equation (9-13) with T in ºC.

$$\sigma_{th} = -0.157 \cdot T + 44.8 \qquad (9\text{-}13)$$

It is interesting to note that if a "fresh" composite Pd-PH structure was taken and pre-treated at 400ºC for one hour in He, its initial microstrains and initial stress were relaxed although its general microstructure was hardly affected (see Figure 9-4 (b)). Moreover, plastic deformations occurred at temperatures higher than 400ºC that also corresponded to temperatures at which significant changes in microstructure were observed as seen in Figure 9-4 (c). The decrease of microstrains at elevated temperatures with minor crystallite growth was also reported in earlier works (Reimann and Wurschum, 1997).

9.4.3 "Extrinsic" stresses upon H_2 loading

9.4.3.1 The determination of n (H/Pd) at T and P

The amount of H_2 absorbed, n (H/Pd), can be determined from Pd lattice parameter using Equation (9-6). However, the use of Equation (9-6) gives n(H/Pd) only up to ± 0.05. All membranes throughout this study were characterized at a maximum H_2 pressure of 5 bar and a minimum temperature of 250ºC. Figure 9-10 shows in blue the pressure/n(H/Pd) region where all membranes were characterized.

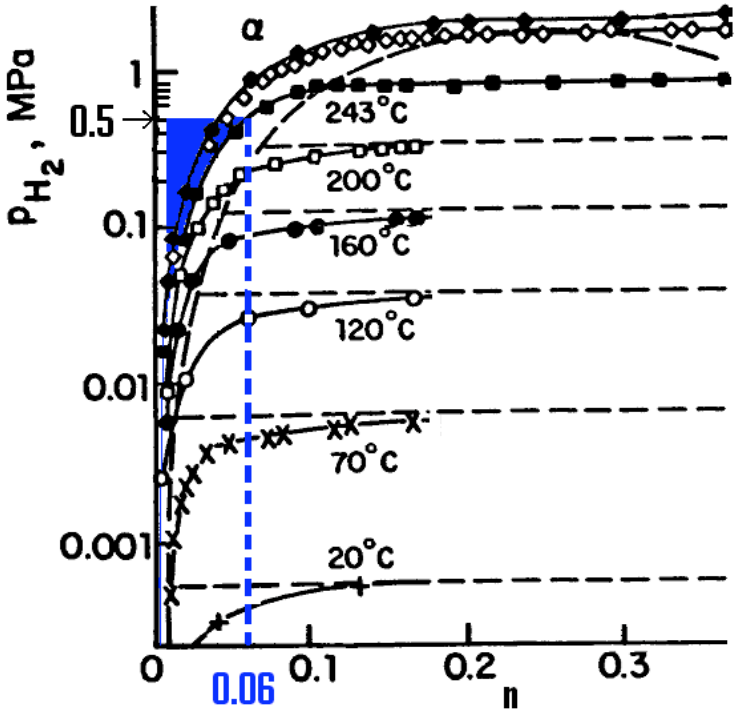

Figure 9-10 Pd-H system in the high pressure and moderate temperature region. The blue dashed line represents the H_2 content (mol H/mol Pd) at 243ºC and an absolute pressure of 5 bar.

The maximum H_2 content, n(H/Pd), was reached at the highest pressure (5 bar) and the lowest temperature (250ºC) and estimated to be 0.06. Hence, any experiment performed with the goal of understanding the influence of H_2 concentration on H_2 stress was carried out at temperature and pressure conditions so that n(H/Pd) would lie within the region of interest (0-0.06). Therefore, due to low accuracy of Equation (9-6) (±0.05) and the narrow window of n(H/Pd) at which the experiments in this section were carried out, the use of Equation (9-6) to determine n(H/Pd) appeared inappropriate.

The H_2 content, n(H/Pd), had to be determined from temperature and pressure values using Sieverts' constant, which relates $P^{0.5}$ to n(H/Pd) by the following linear equation

$$P_{H_2}^{1/2} = K(T) \cdot n(H/Pd) \qquad (9\text{-}14)$$

where K is the Sieverts' constant in $Pa^{0.5}$ or $Torr^{0.5}$ determined from the H_2 absorption isotherm at the temperature T. K was determined for temperatures ranging from 0 to 300ºC from experimental data (H_2 pressure, n(H/Pd)) reported by Gillespie and Hall (1926), Gillespie and Galstaun (1936) and Wicke and Nersnt (1964). The experimental data reported by Gillespie and Hall (1926) and Gillespie and Galstaun (1936) were available in a tabular form so that H_2 absorption isotherms were plotted at 0, 30, 80, 160, 180, 200, 250, 290 and 300ºC and K was determined by considering only the linear portion of $P^{0.5}$ vs. n(H/Pd) as shown in Figure 9-11 for the 30 and 160ºC isotherms. Data of Wicke and Nersnt (1964) were only available in a high quality graph, and K was determined with graphical methods for the 0, 30, 50, 60 and 75ºC isotherms. The natural logarithm of K was then plotted as a function of the inverse temperature for all K values. The resulting Arrhenius type of plot is shown in Figure 9-12. Hence, the H_2 content, n(H/Pd), was determined from the following equation

$$n(H/Pd) = \frac{P^{0.5}}{Exp(\frac{-1114.2}{T} + 9.3)} \qquad (9\text{-}15)$$

with P in torr and T in K. Equation (9-15) in only valid in the stability domain of the α phase and, for a given temperature, in a pressure range where $P^{0.5}$ is a linear function of n(H/Pd).

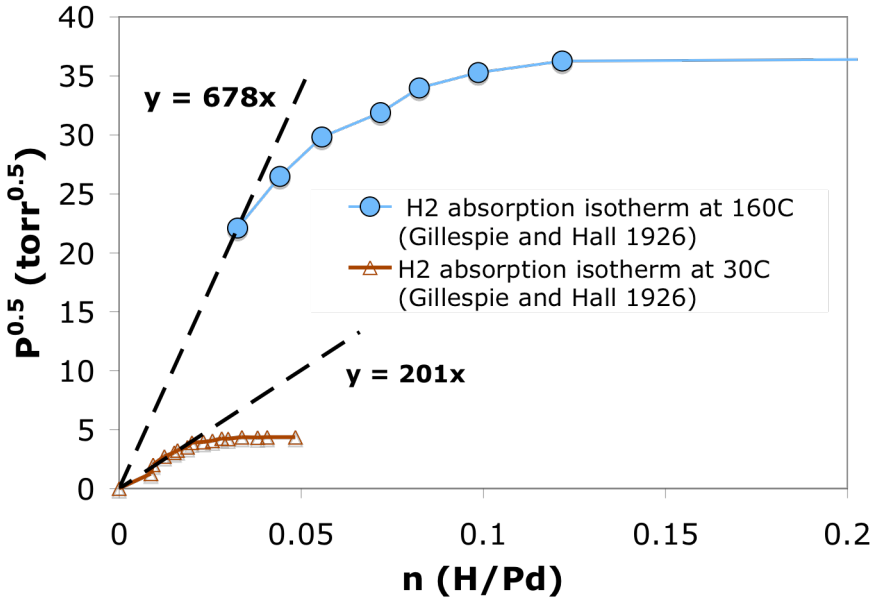

Figure 9-11 $P^{0.5}$ vs. n(H/Pd) at 30 and 160°C. Experimental data from (Gillespie and Hall, 1926).

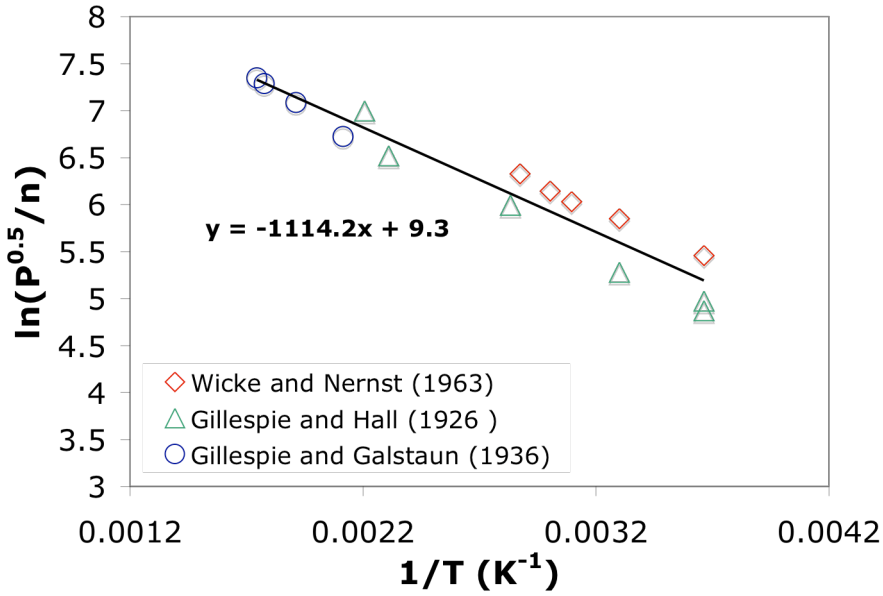

Figure 9-12 Arrhenius plot for $K(=P^{0.5}/n(H/Pd))$ derived from experimental data reported by (Gillespie and Hall, 1926), (Gillespie and Galstaun, 1936) and (Wicke and Nernst, 1964). Temperature range: 0-300°C

Figure 9-13 shows a comparison between H_2 concentration n(H/Pd) determined from 250 and 300ºC isotherms equations reported by Gillespie and Galstaun, (1936) and H_2 concentration, n(H/Pd), determined from Equation (9-15) for the same temperatures and pressures.

The model lines (dashed lines) overestimated by 0.001-0.002 n(H/Pd) the true H_2 concentration at low values of n(H/Pd). At higher pressures, which corresponded to higher values of n(H/Pd), the $P^{0.5}$ vs. n(H/Pd) relation is no longer linear (specially for the 250ºC) and Equation (9-15) underestimates the true value of n(H/Pd).

At each temperature there is a pressure range where the relation P0.5 vs. n(H/Pd) is linear. The higher the temperature the wider the pressure-range within which the relation P0.5 vs. n(H/Pd) is linear. Therefore at temperatures higher than 300ºC the model fits adequately the isotherms as seen in Figure 9-13. The accuracy on the H_2 concentration n(H/Pd) given by Equation (9-15) was estimated to be 0.002, which is significant higher than the accuracy on n(H/Pd) given by Equation (9-6).

9.4.3.2 The presence of compressive stresses upon H_2 loading

The expansion of the Pd lattice as a result of H_2 absorption led to large compressive stresses that can cause a composite Pd membrane to fail. Therefore, it was of great interest to estimate the maximum compressive stresses a composite Pd membrane would be subjected to during membrane characterization and/or membrane operation. This section aims at the fundamental relation between H_2 stress and n(H/Pd).

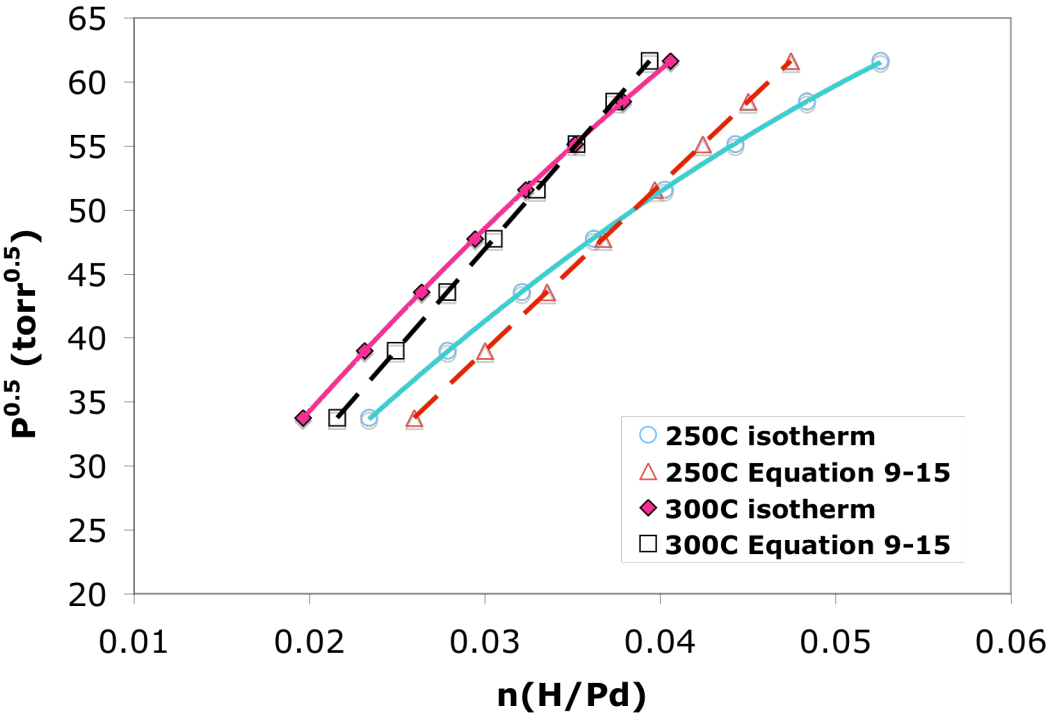

Figure 9-13 Comparison in H_2 concentration n from isotherms and using Equation (9-15)

The total stress of sample PH-1c was measured in a flowing 4% H_2-balance N_2 mixture atmosphere at a temperature of 60ºC and a pressure of 1.5 bar (H_2 partial pressure of 6 kPa). Therefore, the initial H_2 content corresponded to a H_2 solubility c.a. 0.017 (H/Pd) represented by the blue line in Figure 9-14. The use of Equation (9-15) taking P equal to 45.6 torr and T equal to 333K led to n= 0.0177, which supports the validity of Equation (9-15). The total stress of sample PH-1c was then measured at 60, 100, 150, 200, 300 and 500ºC along with the lattice parameter of Pd. Increasing the temperature led to the desorption of H_2 and consequently to the decrease of compressive stresses.

Figure 9-15 shows Pd lattice expansion ($\Delta a/a_0$ in %) as a function of temperature in He atmosphere (open circles) and in the 4%H_2-N_2 balance atmosphere (solid circles). As expected, at 60ºC, the absorption of H_2 led to an expansion of the lattice in addition to the one caused by dilation. As the temperature was increased and the pressure kept constant, H_2 desorbed from the Pd film leading to the asymptotical approach of the lattice parameter to the lattice parameter values measured in He atmosphere. The Pd lattice expansion solely due to the contribution of H_2 content ($(a_H-a_0)/a_0$) was determined by subtracting the contribution of lattice dilation due to temperature from the measured lattice parameter. The H_2 content n(H/Pd) was then determined making use of Equation (9-15) with P equal to 45.6 torr and T ranging from 60 to 500ºC. The values of $(a_H-a_0)/a_0$ were then plotted as a function of n(H/Pd) as shown in Figure 9-16 and fitted with a straight line.

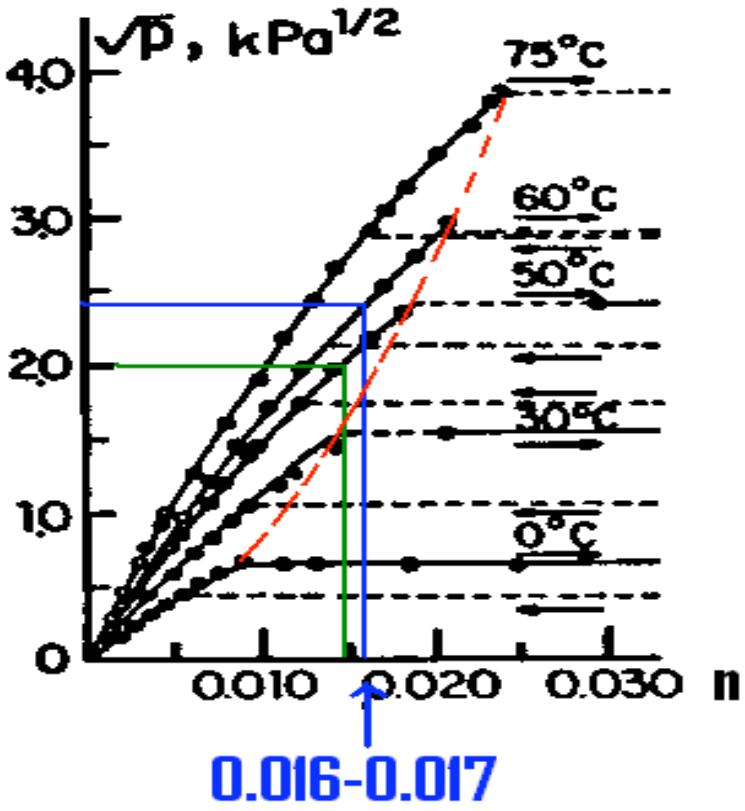

Figure 9-14 Pd-H system in the low pressure and low temperature region. The red line represents the $\alpha/(\alpha+\beta)$ boundary. The blue line represents the H_2 loading (mol H/mol Pd) at 60ºC and an absolute H_2 pressure of 0.06 bars. The green line represents the H_2 loading (mol H/mol Pd) at 50ºC and an absolute H_2 pressure of 0.04 bar.

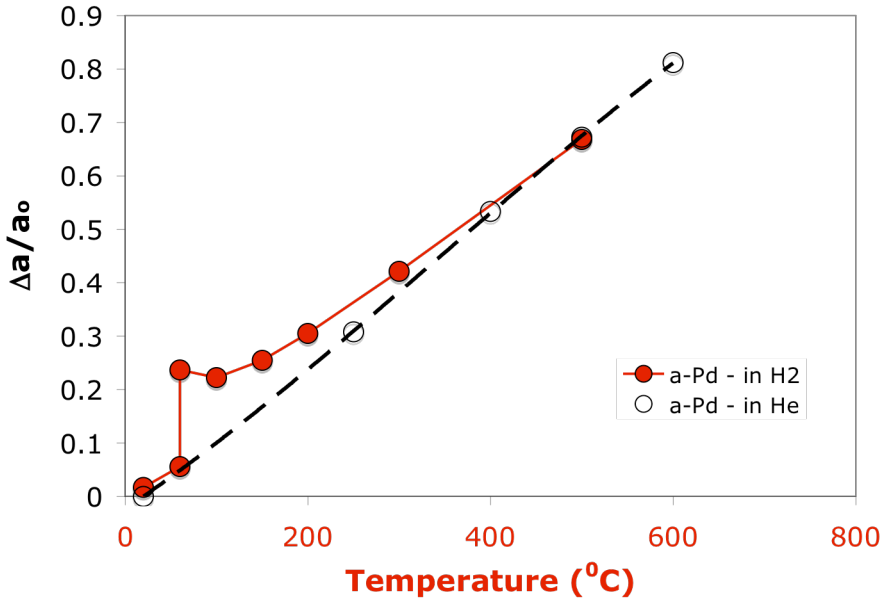

Figure 9-15 Pd lattice expansion due to H_2 uptake and temperature in sample PH-1c

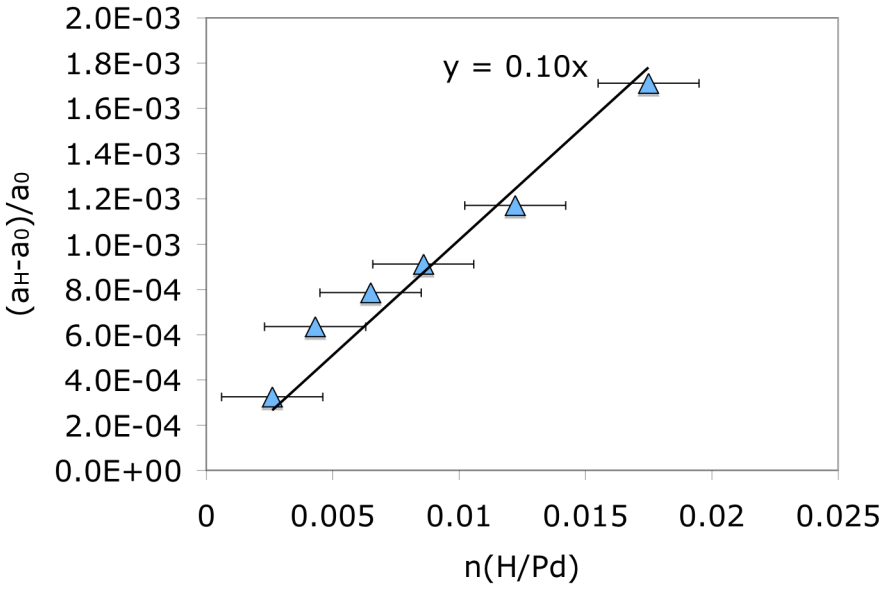

Figure 9-16 Lattice increase due to interstitial H_2 for sample PH-1c.

Pd lattice parameter increased linearly with n(H/Pd) according to Equation (9-16) with a slightly different n(H/Pd) coefficient than Equation (9-6).

$$3 \cdot \frac{a - a_0}{a_0} = 0.30 \cdot n(H/Pd) \qquad (9\text{-}16)$$

Indeed, in this case k_H equals to 0.3 and not 0.19, which is due to the fact that the film is adhered to the substrate and can only expand perpendicularly (Zabel and Hjorvarsson, 2001).

The total stress induced by the Pd lattice expansion due to H_2 loading and thermal stresses is shown in Figure 9-17 for sample PH-1c. H_2 absorption at 60ºC (n=0.017 H/Pd) led to a 0.17% expansion in addition to temperature. The large Pd lattice parameter expansion, constrained by the support, caused the switch from a 40MPa tensile stress in He to a 60MPa compressive stress in H_2 as seen in Figure 9-17. As the temperature was increased the compressive stress slowly decreased from 60MPa at 60ºC to 0MPa at temperatures higher than 200ºC, which corresponded to stress values recorded in He atmosphere. The H_2 stress component was derived by subtracting the elastic thermal stress given by Equation (9-13) from the total measured stress Equation (9-7). The H_2 content, n(H/Pd), was calculated using Equation (9-15) with P equal to 45.6 torr and T ranging from 60 to 500ºC. Figure 9-18 shows the H_2 stress component (σ_H) as a function of n(H/Pd). As expected σ_H was a linear function of n(H/Pd) in the 60-400ºC temperature range. At 500ºC Equation (9-13) was no longer valid due to the stress relaxation by plastic deformations, and the 500ºC experimental data point fell outside the predicted stress line.

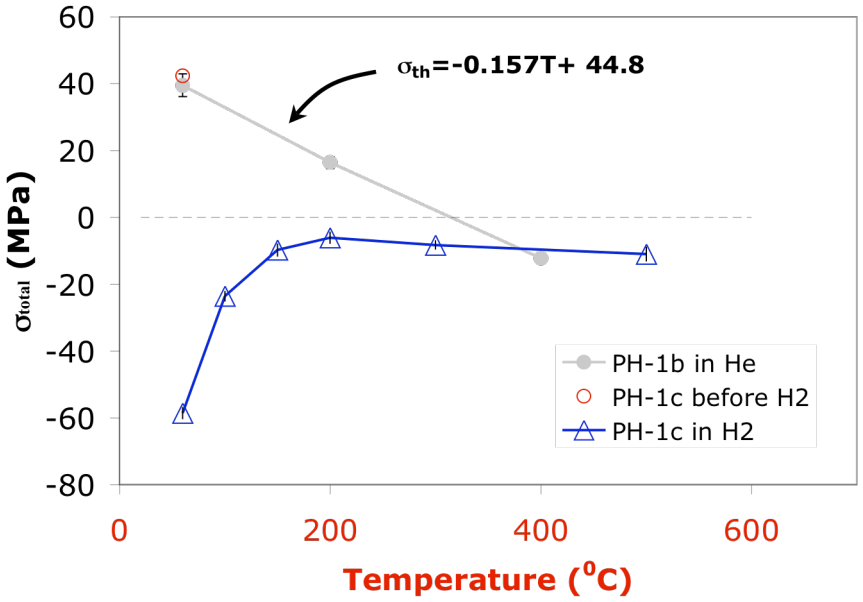

Figure 9-17 Stresses arisen in the Pd thin film due to H_2 uptake

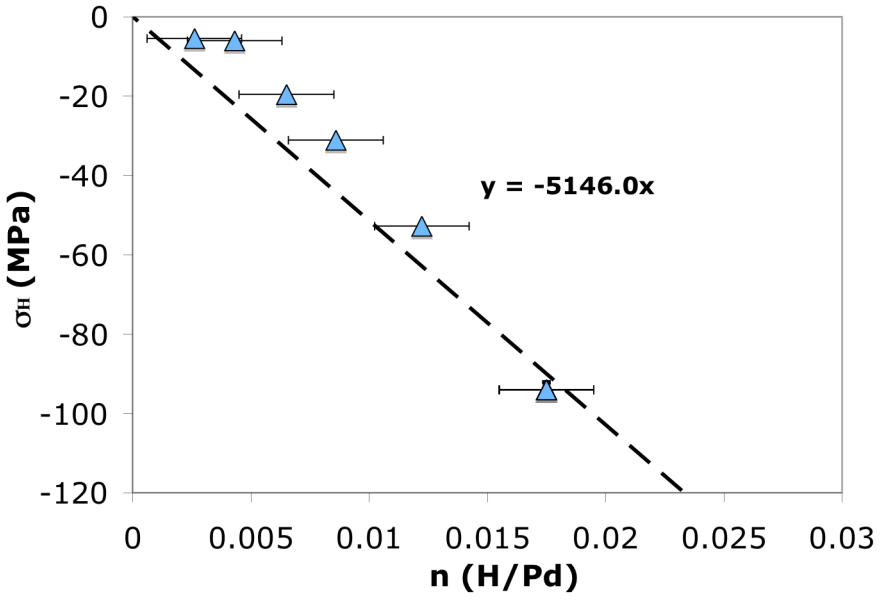

Figure 9-18 H_2 stress as a function H_2 content n(H/Pd)

Therefore, for any composite Pd-PH structure pre-treated at 400ºC, the H_2 stress is given by Equation (9-17)

$$\sigma_H = -5146.0 \cdot n(H/Pd) \quad (9\text{-}17)$$

The total stress in the composite Pd structure is given by the sum of Equation (9-13) and Equation (9-17)

$$\sigma_{total} = -0.157 \cdot T - 5146.0 \cdot n(H/Pd) + 44.8 \quad (9\text{-}18)$$

where σ_{total} is in MPa, T is in ºC and n in mol H/mol Pd. Equation (9-18) is only valid within the elastic region of Pd, which was shown to be 20-400ºC. At temperatures above 400ºC, the elastic energy accumulated in stresses was released by dislocation or grain boundary diffusional creep.

9.4.4 Estimation of stresses during membrane characterization

Knowing the fundamental principles and equations of thermal and H_2 stresses it was possible to estimate the total stress a composite Pd-PH membrane is subjected to by using Equation (9-18). The use of Equation (9-18) implied that the composite Pd membrane was already preanneled in He at 400ºC for one hour. To determine the total stress at 250 and 300ºC, n (H/Pd) was determined by using the experimental isotherms at 250 and 300ºC reported by Gillespie and Galstaun (1936) but also using Equation (9-15) in order to see the differences between the stress values calculated from the model (Equation (9-18)) and those calculated using the Pd-H isotherms.

Figure 9-19 shows the total stress calculated at 250, 300, 400 and 500ºC using Equation (9-15) (dashed lines) and the experimental isotherms from Gillespie and Galstaun (1936) (solid lines).

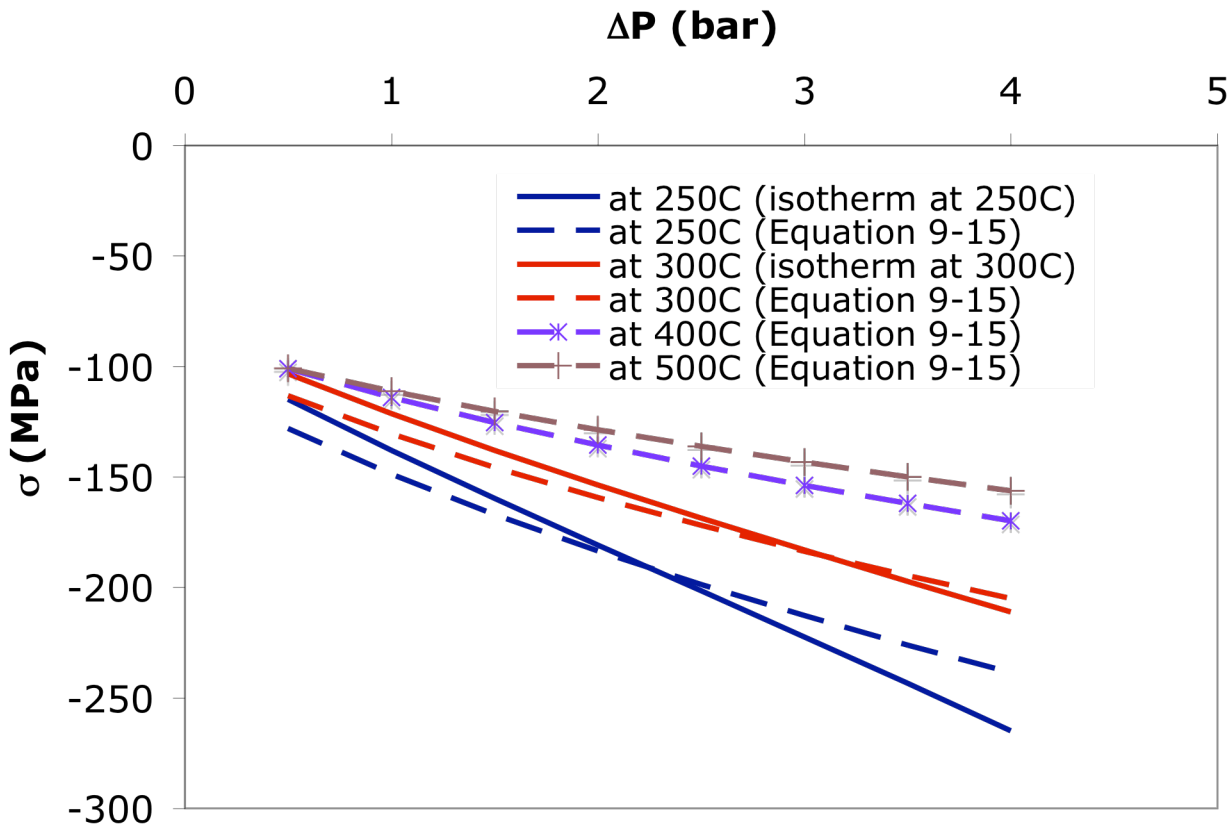

Figure 9-19 Total stress calculations for a Pd composite membrane as a function of pressure difference at 250, 300, 400 and 500ºC. Solid lines at 250 and 300C represent stress calculation using the actual isotherms at 250 and 300C (Gillespie and Galstaun (1936) for the determination of n (H/Pd). Dashed lines represent stress calculations using Equation 5.19 for the determination of n (H/Pd)

In the low pressure range the model overestimates the stress value since Equation (9-15) overstimates n(H/Pd) at low H_2 content values. However, in the high pressure range the model sligtly underestimates the stress value. Moreover, at high pressures and low temperatures, for instance 5 bar at 250ºC, the difference in total stress between the model and the true stress value is quite high (26MPa) since at 250ºC the relation $P^{0.5}$ vs. n is not linear in the 0-5bar pressure range and the model undersestimates the H_2 content. As the temperature is increased to 300ºC, the difference between the model and the true stress value is smaller (6MPa) since at 300ºC the experimental $P^{0.5}$ vs. n(H/Pd) relation could be fitted quite well with a straight line in the 0-5 bar pressure range.

Therefore, the model will always slightly overestimate the stress at low pressure. However, at high temperatures (T>300ºC) Equation (9-15) can estimate the stress very well due to the linearity of $P^{0.5}$ vs. n(H/Pd) in the 0-5 bar pressure range.

Figure 9-19 also shows that a composite Pd-PH membrane pre-annealed at 400ºC will always be under compressive stresses. The calculated stress values at 500ºC are obviously an indication of what would be the stress without relaxation. Indeed, at temperatures higher than 400ºC the elasticity region of Pd is exceeded and stresses relax leading to lower values than the predicted ones. However, experiments on samples PH-1a, PH-2a, PH-3a and especially PH-1c suggested that at 500ºC composite Pd-PH structures were still under small compression stresses. Finally, the maximum stress to which these composite Pd membranes were subjected at 250ºC and 5 bar was estimated to be compressive with a magnitude of 265 MPa (see Figure 9-19).

The experimental data collected for all membranes at 250ºC in He and H_2 atmosphere suggested that holding a composite Pd membrane at 250ºC in H_2 atmosphere did not lead

to leakages. That is, even after excursion up to H_2 pressures equal to 4.5 bar at 250ºC, where compressive stresses are the highest and equaled 260MPa, no leaks were measured in the composite Pd membrane. At 500ºC and at 2 bar H_2 pressure in the shell side the total stress was calculated to be compressive 100MPa if no stress release occurs. Therefore, it appears that stresses do not have a crucial role in leak development.

9.4.5 The effect of atmosphere cycling

During membrane operation, H_2 was introduced at 250ºC at a ΔP of 1 bar, which corresponded to a change in total stress from 6MPa tensile to 150 MPa compressive. It was of interest to understand how critical this change in nature and magnitude of the total stress was to the composite Pd membranes. Figure 9-20 shows the Williamson-Hall plot of sample PH-4a pre-annealed at 400ºC in He for 1 hr. The atmosphere was changed five times at 50ºC using UHP He and 4% H_2-balance N_2 at a 1bar pressure. Therefore, ten sets of data were plotted in Figure 9-20, five in He atmosphere and five in H_2 atmosphere. The experimental temperature and H_2 pressure parameters allowed us to study the introduction of microstrains by changing H_2 concentration in Pd between 0 and 0.015 n (H/Pd) (see green line in Figure 9-14). The changes in the H_2 concentration corresponded to changes in total stress between 40 MPa tensile in He and 40 MPa compressive in H_2.

For the atmospheres, He and H_2, no trend has been seen as a result of cycle number, that is, microstrains or the slope of the lines $\beta \cdot \cos(\theta)$ vs. $\sin(\theta)$ did not increase systematically with cycle number.

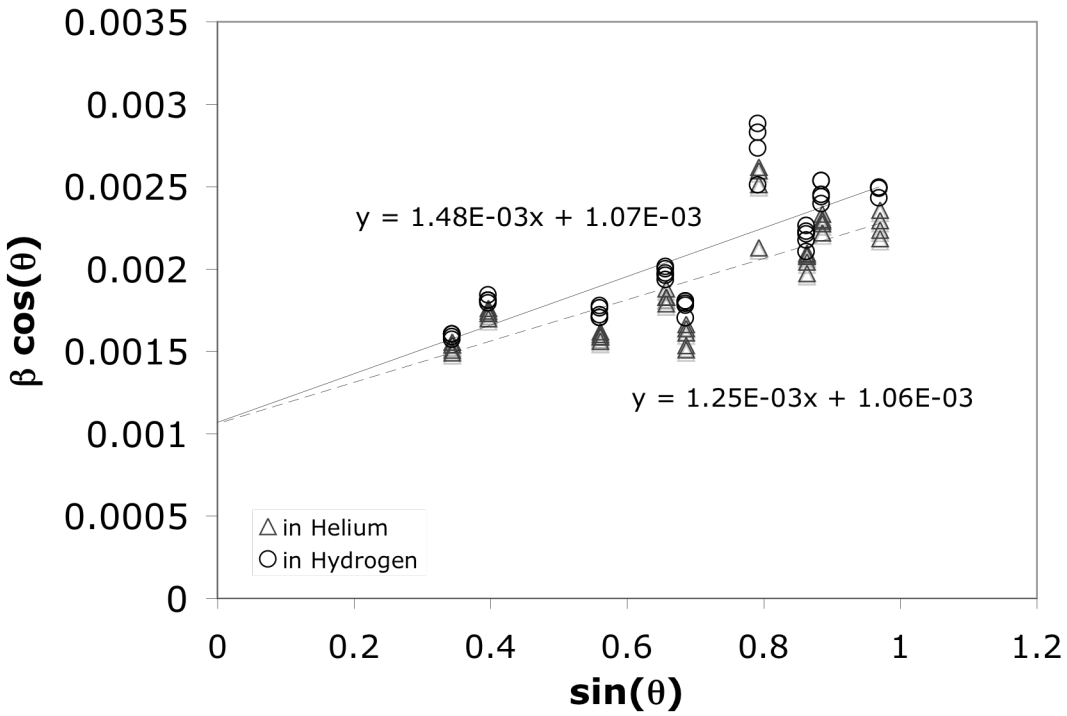

Figure 9-20 Microstrains in He and H_2 atmosphere for sample PH-4a pre-annealed in He at 400°C for one hour

As a consequence, an average microstrains value was estimated for the five H_2 lines and a second microstrains value was considered for the five He lines. As seen on Figure 9-20, the average microstrains (0.025%) in He atmosphere was smaller than in H_2 (0.029%) and both were very small compared to the initial microstrains present in the layer (0.29%).

Consequently, the heat-treatment of Pd thin films at 400ºC for one hour in He led to the irreversible release of microstrains. Once the microstrains were released, even by applying large stresses to the composite Pd-PH structure did not reintroduce microstrains. Microstrains only exist in freshly deposited samples.

9.4.6 Stress measurements in Pd-Cu –PH composite structures

The thermal stresses in composite Pd-Cu-PH were measured for the α phase and the β phase. Figure 9-21 shows the thermal stresses as a function of temperature for samples Pd-Cu-5 and Pd-Cu-6. The H_2 for pure Pd samples was also plotted for comparison purposes. Figure 9-21 shows that Pd-Cu layers on PH were subjected to higher tensile stresses in the 20-400ºC temperature range than Pd layers on PH. Higher tensile stresses in Pd-Cu alloys were consistent with the fact that Pd-Cu alloys have a larger thermal expansion coefficient than Pd. The thermal expansion coefficient of Pd-Cu alloys increases with Cu content, therefore, higher tensile stresses were expected for the Pd-Cu 40wt% (β phase) than for the Pd-Cu 10wt% alloy (α phase). Unfortunately, the thermal stresses on sample Pd-Cu-6 with the Pd-Cu α phase were measured with a low accuracy due to the low 2θ reflection considered. Figure 9-21 also indicates, by extrapolation to higher temperatures, that thermal stresses in the Pd-Cu layer were tensile at 500ºC if no stress release occurred.

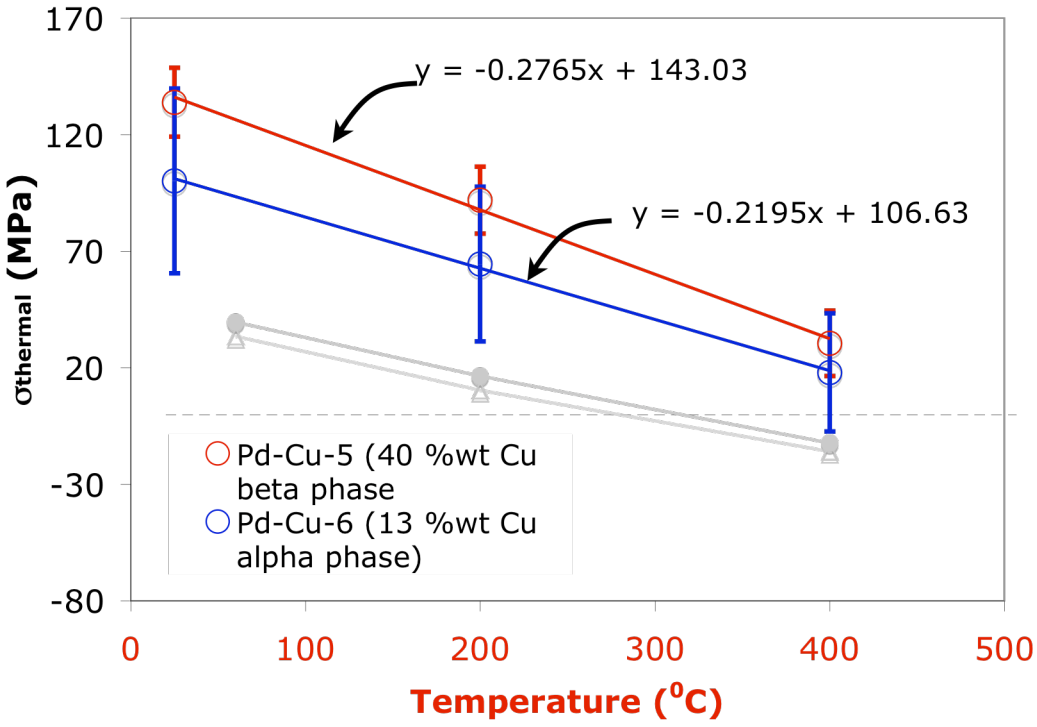

Figure 9-21 Thermal stresses as a function of temperature for the β phase (open circles) and the α phase (open diamonds)

The H_2 solubility in Pd-Cu alloys is very low. For instance, for the same H_2 pressure and temperature, the H_2 solubility is 100 times lower in Pd-Cu 40wt% than in pure Pd (Völkl and Alefeld, 1978). Therefore, H_2 stresses in a composite Pd-Cu 40wt% – PH structure should be 100 times lower than H_2 stresses in a composite Pd-PH structures. The maximum H_2 stress in a composite Pd-PH structures (at T=250ºC and P=4.5 bar) was estimated to be equal to 300MPA, therefore in a composite Pd-Cu 40wt% – PH structure the maximum H_2 stress would be equal to 3MPa. In fact, in composite Pd-Cu-PH structures H_2 stresses are negligible and the total stress equals the thermal stress. Hence, composite Pd-Cu 40wt% – PH structures are subjected to tensile stresses in the 20-400ºC temperature range regardless of the atmosphere. At temperatures higher than 400ºC, thermal stresses may become compressive with further stress release.

9.5 Conclusions

Freshly prepared composite Pd-PH structures were characterized by small Pd grains (50-100nm), an initial tensile intrinsic stress of 104.7MPa and an initial microstrains value of 0.29%. Initial microstrains and stress were released by heat-treatment in He at 400ºC for one hour with no visible change in microstructure. After annealing at 400ºC, thermal stresses were found to be a linear function of temperature in the 20-400ºC elasticity region in agreement with the literature. At temperatures higher than 400ºC stress relaxation occurred with visible changes in microstructure. Pd lattice parameter and H_2 stresses were found to be linear functions of H_2 concentration n (H/Pd) also in agreement with previous works. Stress estimations for pre-treated composite Pd membranes at 400ºC showed that the Pd thin films were always under compressive stresses. During membrane characterization the maximum compressive stress was reached at 250ºC and a

pressure of 5 bar and equaled 265 MPa. In addition stress did not play an important role in leak formation.